Arsenic-fluoride co-contamination in groundwater: Background and anomalies in a volcanic-sedimentary aquifer in central Italy

Daniele Parrone, Stefano Ghergo, Eleonora Frollini, David Rossi, Elisabetta Preziosi

PII: S0375-6742(20)30183-7

DOI: https://doi.org/10.1016/j.gexplo.2020.106590

Reference: GEXPLO 106590

To appear in: *Journal of Geochemical Exploration*

Received date: 14 March 2020

Revised date: 1 May 2020

Accepted date: 6 June 2020

Please cite this article as: D. Parrone, S. Ghergo, E. Frollini, et al., Arsenic-fluoride co-contamination in groundwater: Background and anomalies in a volcanic-sedimentary aquifer in central Italy, *Journal of Geochemical Exploration* (2018), https://doi.org/10.1016/j.gexplo.2020.106590

Arsenic-fluoride co-contamination in groundwater: background and anomalies in a volcanic-sedimentary aquifer in central Italy

Daniele Parrone[a*], Stefano Ghergo[a], Eleonora Frollini[a], David Rossi[a], Elisabetta Preziosi[a]

[a]IRSA-CNR, Water Research Institute - National Research Council, Via Salaria km 29.300, PB 10, 00015 Monterotondo (Rome), Italy

* Corresponding author: parrone@irsa.cnr.it. Tel +39 340 4891370

Stefano Ghergo: ghergo@irsa.cnr.it
Eleonora Frollini: frollini@irsa.cnr.it
David Rossi: rossi@irsa.cnr.it
Elisabetta Preziosi: preziosi@irsa.cnr.it

ABSTRACT

In a volcanic-sedimentary aquifer in central Italy, we investigate the co-existence of arsenic and fluoride in groundwater, aiming at identifying the most probable processes deductible at regional/groundwater body scale leading to the observed co-contamination in groundwater. Further, the areas at risk for human health where high concentrations can produce a significant risk to human health have been investigated.

The study area is located in Latium (Central Italy) where silica-undersaturated alkali-potassic formations of Plio-Pleistocene age largely outcrop above marine and continental sand and clay deposits (Neogene) and continental alluvial deposits (Lower Pleistocene–Middle Pleistocene). Geochemical data from groundwater at 322 wells and 76 springs have been analyzed through statistical methods including clustering/PCA and geostatistical analysis. The results show exceedances of the drinking water standards for F (1.5 mg/L) and As (10.0 µg/L) in 29% and 55% of the sampled groundwater, respectively. Multivariate statistics suggest a widespread process of water-rock interaction with the K-alkaline volcanic formations releasing As, F, K, Si, V, Rb and PO_4 to the groundwater. As and F show a good correlation (Pearson's r = 0.61, Spearman's r_s = 0.59) and define a separate PCA component, confirming that their background in groundwater might be governed by a common process.

Kriging interpolations have been used to study the spatial distribution of the two parameters, identifying areas with the highest concentrations and highest probability of exceeding the standards for human consumption. Moreover, by resampling the As-F data with the jackknife technique it was possible to identify the variations of their correlation index in the study area, due to specific As or F anomalies. While in the peripheral areas of the volcanic districts, dominated by sedimentary deposits, the As-F correlation index does not present important fluctuations, Indicator Kriging shows specific As or F correlation anomalies within the volcanic groundwater bodies and along the Tyrrhenian coastline. These anomalies seem to correspond to the zones with the highest thermal flux and/or are located near important structural lineaments. Fluoride correlation anomalies close to mining sites (fluorite) have also been observed. We hypothesize that, unlike the regional

co-contamination, these local anomalies are related to the upwelling of geothermal fluids along fracture/fault systems that mix with cold groundwater, or to the interaction with mineral deposits particularly enriched of these elements.

Keywords
Water resources management, Contamination, Q-Q plot, Cluster Analysis, Kriging

Highlights

- Arsenic-fluoride correlation in a volcanic-sedimentary aquifer in Italy is analyzed
- Water-rock interaction produces the As-F background and maintains their correlation
- Anomalies appear linked to interaction with geothermal fluids and/or mineral deposits
- Indicator kriging indicates the most suitable areas for drinking water exploitation

1. INTRODUCTION

Arsenic and fluorine are natural elements easily found throughout the environment. Their presence in groundwater depends on the geological setting as well as on various natural processes, including climate, biological activity and volcanic emissions. Arsenic and fluoride in drinking-water represent a hazard for human health (WHO, 2017). Long-term exposure to As-rich waters can cause serious diseases, from skin lesions, cardiovascular diseases, type II diabetes to bladder, lung and skin cancers (Cubadda et al., 2015, Karim, 2000; Rossman et al., 2004; Tchounwou et al., 2004; Yoshida et al., 2004). An excessive intake of fluorine can cause dental and skeletal illness (fluorosis), although at low concentration (about 0.6 mg/L) it preserves teeth and bones (Brindha and Elango, 2011). In groundwater these two elements frequently show concentrations exceeding the guideline values suggested by WHO (2017) as drinking water standards (10.0 µg/L for As, 1.5 mg/L for F) and retained by the European legislation (98/83/EC), entailing an important risk to human health.

Since the recognition in the 1990s of its wide occurrence in well-water in Bangladesh, the origin and fate of arsenic in groundwater has attracted the attention of the scientific

community (e.g. Anawar et al., 2003; McArthur et al., 2004; Nickson et al., 2000; Smedley and Kinninburgh 2002). Water–rock interaction under favorable biogeochemical conditions is by far considered the most important mechanism for the presence of arsenic in groundwater (Mukherjee et al. 2014); its concentration in natural waters may range from 0.5 to more than 5000 µg/L (Smedley and Kinniburgh, 2002). Arsenic-enriched groundwaters have been reported in many parts of the world (BGS, 2019a), mainly in Asia (Bangladesh, China, India, Vietnam, Nepal), America's (USA, Mexico, Argentina, Chile, etc.) and Europe (Achene et al., 2010; Bundschuh et al., 2012; Ford et al., 2006; Nicolli et al., 1989, 2012; Pazand and Javanshir 2013; Rango et al., 2013; Yang et al., 2009; Vivona et al., 2007). Mukherjee et al (2014) have hypothesized a relation between the large scale geodynamic processes and the distribution of As-enriched groundwater, as the contaminated areas are often part of large sedimentary basins adjoining major orogenic belts. In the Italian active volcanic systems, arsenic in groundwater ranges between 0.1 and 7000 µg/L, with the highest values detected in fracture zones where hot hydrothermal fluids may promote water-rock interaction and the dissolution of As-bearing sulphides (Aiuppa et al., 2003; Daniele, 2004).

Fluoride concentration in groundwater varies greatly and can reach several tens of mg/L depending on the geological settings, rock type, climate (arid regions are prone to high fluoride concentrations) and reaction times with aquifer minerals (Brunt et al., 2004). In volcanic areas where hydrothermal processes are still active, high concentration of fluoride in groundwater is common (Edmunds and Smedley, 2013). Since fluoride can derive from different rock types, concentrations up to some tens of mg/L have been detected in diverse geological environments and in several countries worldwide (Armienta and Segovia, 2008; Brindha and Elango, 2011; Brunt et al. 2004). At the global scale, the documented areas with high-fluoride groundwater (Edmunds and Smedley, 2013) partly overlap with the As-laden groundwater (Smedley 2008), but extends over a much larger part of Africa, where

East African Rift Valley represents one of the most significant high-fluoride provinces in the world (BGS, 2019b).

The scientific literature is abundant regarding the co-presence of arsenic and fluoride and the main processes leading to their release in groundwater (Claesson and Fagerberg, 2003; Kim et al., 2012; Nicolli et al., 2001; Smedley et al., 2002). Alarcón-Herrera et al. (2013) found that the co-occurrence of these contaminants in Latin America is common especially in oxidized and alkaline environment, their primary sources being volcanic glass and, to a lesser extent, hydrothermal minerals. Further, they identified Fe-, Mn-, and Al-(hydr)oxides as secondary sources, due to the great adsorption affinity of As and F. Other authors claimed that the desorption from Fe-(hydr)oxides is the major process for As-F co-contamination (e.g. Kim et al 2012), where their correlation is generally very good because the As released from Fe-(hydr)oxides does not readily precipitate again. In oxidizing conditions, a good correlation between arsenic and fluoride has been observed e.g. in Argentina (Bhattacharya et al., 2006; Gomez et al., 2009), California (Levy et al., 1999) and Italy (Vivona et al 2007). In Argentina, Francisca and Carro Perez (2009) reported the presence of arsenic, fluoride and vanadium in groundwater due to volcanic glass leaching. In a volcanic aquifer in Mexico, under oxidative conditions and high temperature, Morales et al. (2015) observed a good correlation (0.76) between As and F, whose mobilization from metallic sulfides (As) and from primary minerals of deep rhyolite units (F), would be favored by thermal water rising through faults and fractures. Currell et al. (2011) found a strong positive correlation between the ratios F/Cl and As/Cl in the groundwater of the Yuncheng Basin, China, and concluded that these elements are mobilized and enriched by common processes including de-sorption of As and F anions from Fe-, Mn-, and Al-(hydro)oxides. Vivona et al. (2007) reported a fair correlation between arsenic and fluorine in the K-alkaline volcanic aquifer of central Italy, mostly in oxidizing conditions, and

hypothesized that the precipitation of fluoroapatite, due to calcium increase along the flow path, was governing the thermodynamic equilibrium.

In reducing conditions, on the other hand, the correlation of As and F seems to be missing. For example, Guo et al. (2012), further to the large spatial variation of both arsenic and fluoride in groundwater of a superficial alluvial-lacustrine aquifer and increasing concentration of As with depth, did not observe any significant correlation between As and F concentration. They attributed As release to the reductive dissolution of Fe oxides, while they linked fluoride to the dissolution-precipitation of Ca minerals (fluorite and calcite) and adsorption-desorption phenomena in arid environment. Kim et al. (2012) suggested that the poor correlation between the two elements in reducing aquifers is due to the fact that arsenic released through the reductive dissolution of Fe-(hydr)oxides can be easily removed from the groundwater when the reduction of sulphates to sulphides occurs, while fluoride concentrations are independent of the same reaction.

In the mainly oxidized and alkaline volcanic aquifers of northern Latium (central Italy), the presence of arsenic and fluoride has been known for many decades (Angelone et al., 2009; Baiocchi et al., 2013; Dall'Aglio et al., 2001; De Rita et al., 2012; Preziosi et al., 2005, 2010; Vivona et al., 2004, 2007). However, it is still unclear which the main origin of the contamination is, nor whether a common process associates arsenic and fluoride. Vivona et al. (2007) claimed volcanic rock leaching in cold groundwater, while Angelone et al. (2009) and De Rita et al. (2012) pointed to a major influence of localized thermal fluids rising along fractures. Armiento et al. (2015) and Cinti et al. (2015), in the same region, ascribed the diffuse As concentration in groundwater to water–rock interaction processes, locally enhanced by thermalism and volcanic gas emissions.

This paper aims to provide an overview on the co-presence of As and F in the large volcano-sedimentary aquifer of northern Latium (central Italy), based on a large amount of data collected in a time span of 16 years. We try to explain the available information using

(geo)statistical methods, identifying the geochemical background, the risk areas and the geochemical anomalies. The co-contamination of As and F is examined at the groundwater body scale, enhancing the anomalies in the As-F correlation: the deviations from the regional correlation are then highlighted and analyzed in relation to the tectonic structures and mineral deposits.

2. DATA AND METHODS

2.1. Case study description: geological and hydrogeological setting

The North-Western sector of Latium (Central Italy) features undersaturated alkali-potassic volcanic deposits, belonging to three different districts (Vulsino, Cimino-Vicano and Sabatino district) (Peccerillo, 2005). The Latium volcanism is related, according to several authors, to the opening of the Pliocene Tyrrhenian back-arc basin (Finetti and Del Ben, 1986) or, as suggested by others, to the development of an upwelling mantle dome during the Miocene - Early Pliocene interval (Locardi, 1982; Wezel, 1982). During the extensional regime, which developed from Middle Miocene to recent, grabens and semigrabens developed in the sedimentary pre-volcanic units (Cretaceous–Eocene flysch sequence and Meso-Cenozoic limestones), delimited by synthetic high-angle normal faults arranged in a westward stepwise pattern. The structural depressions were filled with up to 2000 m thick Neogene neo-autochthonous sequence (marine and continental sand and clay deposits, Cinti et al., 2011). Quaternary continental alluvial deposits (Lower Pleistocene–Middle Pleistocene) and the above mentioned alkali-potassic volcanic deposits subsequently covered this buried configuration. Tectonic lineaments oriented NE-SW and NW-SE linked to the Tyrrhenian extensional tectonic regime controlled the volcanic activity.

The target of this study is a regional water table aquifer (Fig. 1) hosted mainly in the volcanic formations and, towards the southern and eastern borders, in the Quaternary alluvial deposits underlying the volcanites (Boni et al., 1988; Cinti et al., 2011; Dall'Aglio et al., 1994).

The impervious Cretaceous–Eocene flysch sequence and the Neogene clays and sandy-clays, separate this regional aquifer, largely exploited for irrigation, industry and human consumption, from a deeper geothermal reservoir hosted in the thick sequence of the Meso-Cenozoic fractured limestones. As a part of the Central Italy peri-Tyrrhenian volcanic belt, in response to the tectonic setting associated with the opening of the Tyrrhenian Sea, the study area features numerous thermal springs and CO_2 gas emissions (Cinti et al., 2011; Dall'Aglio et al., 1994).

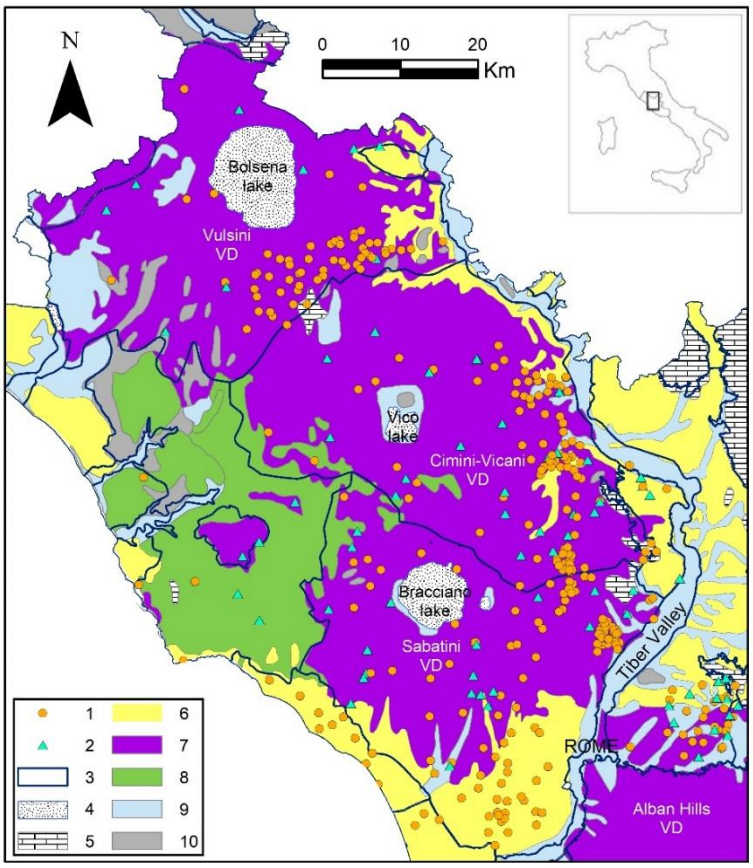

Fig. 1 - Map of the hydrogeological complexes and sampling point location (VD: Volcanic District). Legend: 1 - Wells; 2 – Springs; 3 – Groundwater bodies boundary; 4 – Lakes; 5 – Limestones (Meso - Cenozoic); 6 –

Continental and marine detrital formations (Plio - Pleistocene); 7 – Volcanites (Plio - Pleistocene); 8 - Flysch (Upper Cretaceous - Eocene); 9 – Alluvial deposits (Holocene); 10 – Sterile zones.

2.2. Field and laboratory sampling methodology

A total of 398 groundwater samples were collected by IRSA-CNR (Water Research Institute-National Research Council) from wells (322) and springs (76) tapping the regional water table aquifer between the years 2001 and 2017. Springs fed by small, perched groundwater bodies, as well as hot springs fed by the deep hydrothermal circulation were excluded. These data are the results of sampling activities related to numerous local studies conducted in the region using the same sampling procedures and laboratory protocols. Due to this, the density of the water points is not homogeneous across the study area. The stability of the chemical composition of groundwater across this time span was demonstrated by comparing the chemical composition of some water points which have been sampled more than once, and they do not show significant variations of chemistry (Preziosi et al. 2016; Parrone et al. 2019). All samples were filtered in the field with 0.45 µm polycarbonate membrane filters, in N_2 pressure (Bangsund et al., 1994; Pohlman et al., 1994) and stored in HNO_3 washed polyethylene bottles. One fraction was treated with the addition of HNO_3 to pH < 2 for major cations and trace elements determination. At each site, pH, EC (electrical conductivity), ORP (oxidation-reduction potential), DO (dissolved oxygen) and T (temperature) were measured with probes. Bicarbonates were determined in the field by HCl titration on 1 ml of sample or in laboratory on 50 ml of sample (within 24 hours). The samples were analyzed for anions by ion chromatography (IC, Dionex DX-120), for major cations by Inductively Coupled Plasma - Optical Emission Spectrometry (ICP-OES, Perkin Elmer P400) and trace elements by Inductively Coupled Plasma Mass Spectrometry (ICP-MS, Agilent technologies 7500c); certified materials (NIST 1640a, trace elements in natural waters) were used to check the quality of the laboratory results. Non-

detect data (only for phosphates, DL = 0.005 mg/L, ND<15%) were given a constant value, equal to the half of the limit of detection (USEPA, 2002).

Chemical analysis for major ions have been validated using the electrical balance (E.B.) (EB% < 5%, Appelo and Postma, 2005), calculated applying the equation [1]:

$$EB\% = 100 \cdot \frac{(\sum cations - \sum anions)}{(\sum cations + \sum anions)} \quad [1]$$

Analytical data accuracy for ICP-MS and ICP-OES analysis was tested against certified reference material (NIST 1640a, trace elements in natural waters).

2.3. Statistical treatment of data and geospatial analysis

In addition to univariate and bivariate statistics, multivariate techniques such as hierarchical clustering (using the Unweighted Pair-Group Average algorithm and the correlation as similarity measure) and Principal Component Analysis were applied to group the data and identify linkages between the analyzed elements. The correlation between As and F was represented using scatterplots. Normality or lognormality of the datasets was verified using the Shapiro-Wilk test (1965). Q-Q plots were realized to analyze the geochemical populations, facies variations and possible outliers. Q–Q plots are commonly used to compare a data set to a theoretical model in order to provide a graphical assessment of "goodness of fit". The alignment of the points against the normal theoretical quantiles may suggest the presence of a single statistical population, while any abrupt variation in the distribution of data may indicate the transition between different populations, hence the existence of overlapping geochemical phenomena that determine the overall distribution of data. Data processing was performed through different statistical software: Statistica 7.0 (StatSoft Inc., 2004) for scatterplots and box plots, Past 3.01 (Hammer et al., 2001) for hierarchical clustering and PCA analysis, ProUCL 5.0 (Singh and Maichle, 2013) for Q-Q plots and goodness of fit tests.

Natural phenomena in groundwater often show a certain spatial variability, for which it may be useful to study the distribution and spatial correlation of some chemical parameters. In geostatistics the concept of spatial correlation between the observations is represented by the variogram (or semivariogram), which is a graph illustrating the mean variability between samples vs. the distance separating them. The variogram can be calculated using the expression [2]:

$$y(h) = \frac{1}{2N_h}\sum_{i=1}^{N_h}[z(x_i) - z(x_{i+h})^2] \quad [2]$$

where *h* (lag) is the vector that depends on the direction in which the variogram is calculated, $z(x_i)$ and $z(x_{i+h})$ are the experimental values of the variable *z* measured in the points x_i and x_{i+h}, respectively, and N_h is the number of pairs of points separated by the lag *h*.

Kriging is a geostatistical interpolation technique that assumes the presence of a spatial correlation between the measured values, estimated through the construction of the variograms. Different types of techniques allow performing Kriging: in particular, we applied Ordinary and Indicator Kriging for the interpolation of As and F concentration data.

Ordinary Kriging is one of the most common estimator used to interpolate spatial data, a standard method in environmental science (Gaus et al., 2003; Lin et al., 2002). We used Ordinary Kriging to estimate the distribution of As and F concentrations; the goodness of the spatial interpolation was evaluated by standardized error.

Indicator Kriging is an interpolation method primarily used to estimate the probability of exceeding some predefined threshold. It is based on the data transformation, producing a dataset of binary values: using a specific threshold, original data are transformed into coded values, generating a new indicator variable. This variable is set to 0 for all the concentration values below or equal to the threshold and to 1 for higher concentrations. Applying Indicator Kriging to the coded values allows then to obtain a map where values

range between 0 and 1, which represents the probability of exceeding the threshold value in non-sampled locations of the investigated area. We assumed as threshold values the WHO drinking water standards (10.0 µg/L for As and 1.5 mg/L for F), identifying the areas of northern Latium where, on the basis of the considered datasets, the probability of exceeding the threshold values in groundwater is higher, indicating a higher risk for the human health too.

The jackknife resampling technique is an effective method for detecting data outliers in bivariate statistics (Efron and Stein, 1981; Quenouille 1949, 1956; Tukey 1958). When it is applied to the correlation coefficients, it recalculates the *r* value excluding a couple of data at each step, obtaining a new dataset of correlation coefficients (*r'*) for (n-1) couples. It is apparent that higher values of r' correspond to those samples that are less correlated to the whole, whose elimination involves an important correlation index improvement. This technique has been applied to the As-F dataset and the obtained *r'* dataset was then interpolated through Indicator Kriging. We used the 75th percentile of the r' distribution (0.608) as threshold, thus highlighting the zones where the two parameters result less correlated (higher probability of exceeding the threshold), in order to identify specific As or F anomalies in the study area.

Prior to the interpolation, to overcome the lack of homogeneity of the water points along the study area, the data were de-clustered using the polygons of influence around each point location. The de-clustering weight assigned to each point was calculated as the ratio of its polygon area to the entire area of interest. All the geospatial interpolations have been realized using the software ArcGIS 10.2.2.

3. RESULTS AND DISCUSSION

3.1. Groundwater classification and statistical analysis of data

Main statistics for the field parameters and the analyzed major and minor compounds are reported in Table 1. Many of the considered compounds show an extremely wide concentration range, up to three orders of magnitude, due to the heterogeneous hydrogeological and hydrogeochemical conditions that characterize the study area. Only Si shows low variability and a symmetric (normal) distribution, HCO_3, Ca and Zn are lognormally distributed, while Fe and Mn, which are strongly linked to the existence of reducing environments, are the most variable elements and did not pass the Shapiro Wilk test. Oxidizing redox conditions are largely dominant (over 90% of samples shows positive ORP values), while pH generally remains around neutral values. Fluorine presents variations of almost two orders of magnitude and the 29% of sampled waters shows concentrations exceeding the drinking water limit of 1.5 mg/L. More than half of the samples (55%) exceeds the drinking water standard for As (10.0 µg/L), however, only 3% of samples exceeds 50 µg/L which was the standard limit used before 2003. The highest value observed for arsenic was 128 µg/L, while Angelone et al. (2009) and Cinti et al. (2015) reported much higher values in the same region (371 µg/L and 610 µg/L respectively), although measured in thermal waters.

Parameter	Samples	Min	Max	Mean	Median	VC%	Skewness	Kurtosis
ORP (mV)	385	-323	669	188	200	0.5	-0.3	3.9
T (°C)	398	5.3	25.7	16.6	16.5	0.1	0.0	3.5
pH	396	5.4	8.6	7.0	7.1	0.1	-0.6	0.0
DO (mg/L)	397	0.0	21.3	6.7	7.2	0.5	0.1	0.9
Cond (µS/cm)	317	216	2930	695	597	0.6	2.8	10.3
F (mg/L)	398	0.1	6.1	1.2	1.0	0.8	1.7	3.7
Cl (mg/L)	398	4.2	619.0	37.4	24.0	1.4	6.6	57.5
NO_3 (mg/L)	398	0.1	244.9	25.6	16.6	1.2	3.8	20.0
PO_4 (mg/L)	352	0.003	4.2	0.4	0.3	1.3	2.7	10.5
SO_4 (mg/L)	398	2.0	1018.6	41.6	17.1	2.0	6.3	58.8
HCO_3 (mg/L)	398	31.4	1281.0	288.5	246.4	0.6	2.0	7.2
Na (mg/L)	398	2.5	548.7	38.0	27.8	1.0	6.9	73.1
Mg (mg/L)	398	2.6	132.0	15.6	12.0	0.9	3.5	18.9
K (mg/L)	398	0.2	209.2	27.2	23.4	0.9	3.1	16.6
Ca (mg/L)	398	1.8	420.9	69.7	48.6	0.9	2.3	6.9
Si (mg/L)	364	2.0	58.3	28.9	28.9	0.4	0.0	-0.3
Mn (µg/L)	371	0.02	3577.7	88.7	2.3	3.9	6.5	49.3
Fe (µg/L)	337	0.3	7614.0	187.5	16.4	4.4	6.5	44.2
As (µg/L)	398	0.1	128.5	14.4	11.0	1.0	2.9	14.0
Rb (µg/L)	365	0.2	313.8	53.5	45.2	0.8	2.4	8.1
V (µg/L)	398	0.1	99.4	19.8	16.5	0.8	1.1	1.7
Zn (µg/L)	395	0.2	2470.0	54.8	14.8	3.2	9.5	112.1

Table 1 – Main statistics for the considered parameters.

Groundwater samples show a gradual chemical facies variation from bicarbonate-alkaline to bicarbonate-earth-alkaline facies, corresponding to the transition from volcanic formations to alluvial deposits (Fig. 2), as already observed by Parrone et al. (2013), Preziosi et al. (2014) and Vivona et al. (2007). The samples from the volcanic deposits (gray triangles and white dots) are more alkaline due to the presence of K, while those collected in the ancient alluvial sediments downstream, on the border of the volcanic districts (black squares), are increasingly calcium-bicarbonate type due to the interaction of groundwater with the mainly calcareous alluvial sediments.

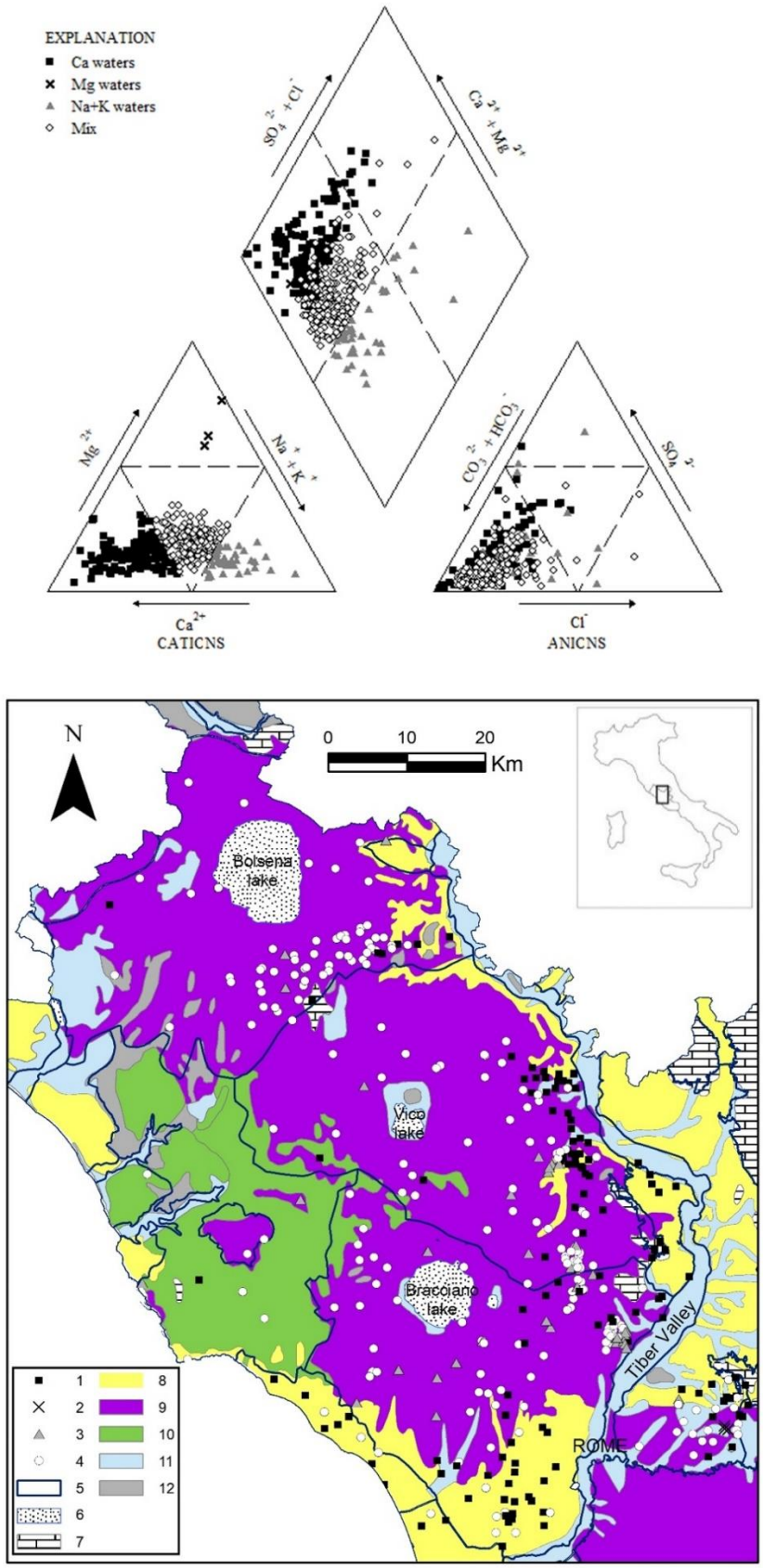

Fig. 2 - Hydrochemical classification of groundwaters on the Piper diagram and map of the hydrogeological complexes. Sampling points are distinguished on the basis of the dominant cation, adopting the same

symbols of the Piper diagram. Legend: 1 – Ca waters; 2 – Mg waters; 3 – Na+K waters; 4 – Mix; 5 – Groundwater bodies boundary; 6 – Lakes; 7 – Limestones (Meso - Cenozoic); 8 – Continental and marine detrital formations (Plio - Pleistocene); 9 – Volcanites (Plio - Pleistocene); 10 - Flysch (Upper Cretaceous - Eocene); 11 – Alluvial deposits (Holocene); 12 – Sterile zones.

The good bond between As and F (Fig. 3) is confirmed by the values of the correlation coefficients (Pearson's r = 0.61; Spearman's r_s = 0.59; Significance level: 0.001), suggesting that a common geochemical process is governing the origin and/or fate of the two elements in groundwater. Good correlation of As and F has been observed also in other parts of the world and in different types of aquifers in oxidizing conditions (Currell et al., 2011; Guo et al., 2012; Kim et al., 2012), but a convincing explanation for this has not been provided so far.

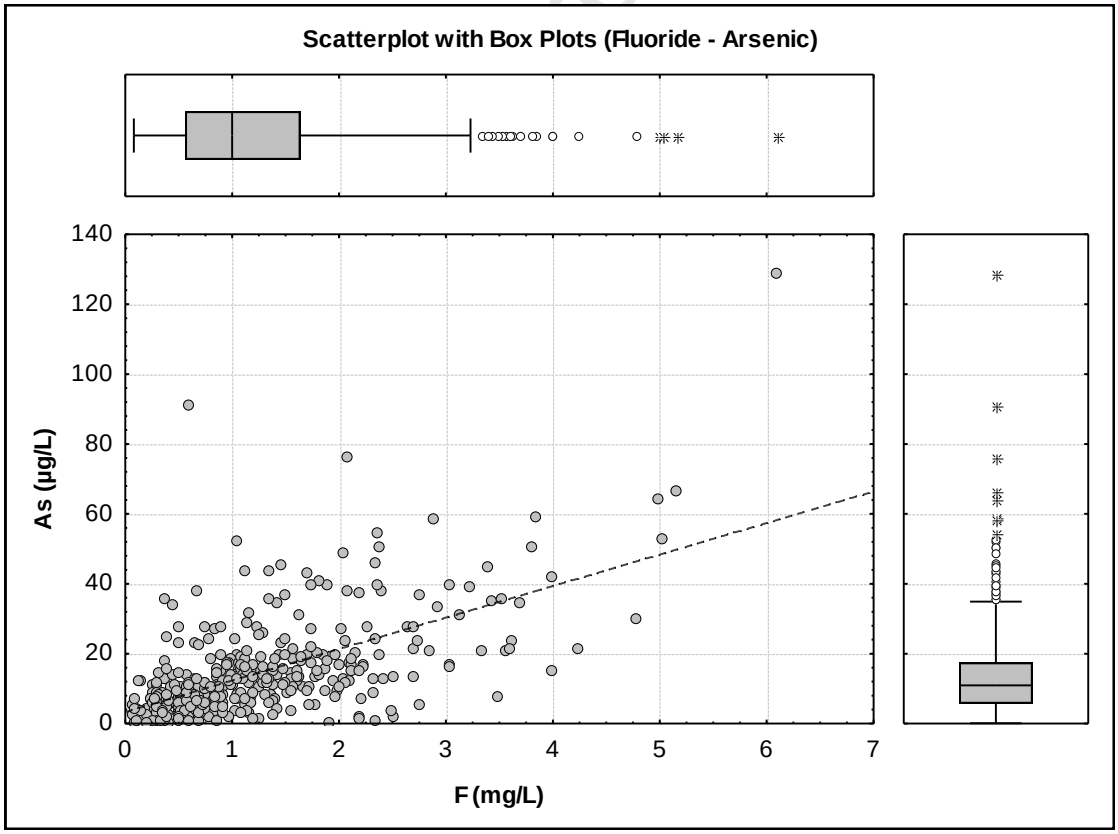

Fig. 3 – Scatterplot F-As and box plots for the two parameters.

In addition, As and F show moderate positive correlation with K, Rb and V (Table 2). The reductive dissolution of Fe oxides/hydroxides is one of the processes responsible for the As release to groundwater, particularly in reducing conditions (Preziosi et al. 2019). However, in the study area the lack of correlation between As and Fe points at a poor control by Fe oxides/hydroxides on the As mobility. These minerals are not included in the paragenesis of pyroclastic flows, while sulfides could be a major source for arsenic and fluorite and fluorapatite could be important reservoirs for fluoride.

	F	Cl	NO_3	PO_4	SO_4	HCO_3	Na	Mg	K	Ca	Si	Mn	Fe	Rb	V	Zn	As
F																	
Cl	-0.17																
NO_3	-0.20	0.17															
PO_4	**0.21**	**-0.35**	0.11														
SO_4	-0.14	**0.61**	0.13	**-0.21**													
HCO_3	-0.12	**0.57**	-0.18	**-0.37**	**0.55**												
Na	0.07	**0.73**	0.01	-0.19	**0.62**	**0.66**											
Mg	**-0.24**	**0.57**	0.05	-0.09	**0.61**	**0.70**	**0.62**										
K	**0.61**	**-0.21**	**-0.25**	**0.40**	-0.16	-0.08	0.07	-0.12									
Ca	**-0.28**	**0.63**	0.01	**-0.41**	**0.62**	**0.89**	**0.59**	**0.64**	**-0.28**								
Si	**0.29**	**-0.36**	0.06	**0.71**	**-0.22**	**-0.36**	-0.16	-0.10	**0.54**	**-0.43**							
Mn	0.08	0.11	**-0.32**	0.02	**0.28**	**0.32**	**0.29**	**0.30**	**0.22**	**0.25**	0.09						
Fe	0.05	0.12	**-0.20**	-0.07	**0.26**	**0.22**	0.17	**0.21**	0.12	**0.21**	-0.03	**0.56**					
Rb	**0.39**	**-0.36**	-0.01	**0.51**	**-0.21**	**-0.32**	-0.13	**-0.22**	**0.58**	**-0.37**	**0.59**	0.09	0.01				
V	**0.35**	**-0.30**	**0.23**	**0.58**	**-0.44**	**-0.42**	**-0.23**	**-0.24**	**0.37**	**-0.47**	**0.49**	**-0.25**	**-0.23**	**0.34**			
Zn	0.03	0.14	0.09	-0.10	0.13	0.11	0.11	0.09	0.00	0.14	-0.12	**0.24**	0.18	-0.03	-0.15		
As	**0.59**	**-0.26**	-0.17	**0.30**	**-0.29**	**-0.27**	-0.03	**-0.42**	**0.46**	**-0.37**	**0.33**	-0.01	-0.07	**0.44**	**0.42**	-0.09	

Table 2 – Spearman (r_s) correlation coefficients for the analyzed parameters. Statistically significant values in bold (α = 0.001).

Hierarchical Clustering (Fig. 4) highlights the presence of distinct groups of compounds. The first one includes the major ions (with the exception of K) which are well correlated to each other. The second cluster includes K, Si, PO_4 and some minor elements such as F, As, Rb and V. Finally, Mn and Fe are clustered together while NO_3 and Zn are isolated. The first cluster (major ions) mainly characterizes the groundwater sampled in the peripheral zones of the investigated area, where the contribution of the sedimentary deposits to water chemistry becomes more important (black squares in Fig. 2). In contrast, the second cluster includes compounds that are characteristic of the K-alkaline volcanic

formations and seems to identify the contribution of the volcanic products to the chemistry of groundwater in the inner part of the aquifer (white dots and grey triangles in Fig. 2). The isolation of NO_3 and Zn from the other compounds underlines that they might be due to other phenomena not related to the water-rock interaction.

In the Principal Component Analysis, PC1 and PC2 (explaining the 22.9% and 17.0% of the total variance) highlight the presence of the two main groups already mentioned for the cluster analysis. In particular, PC1 shows very positive loadings for the major ions, while the second component features a positive contributing factor for the elements included in the second cluster, the latter indicating the contribution of the volcanic formations to the chemistry of groundwater. The PC3 (10.9% of the total variance) shows positive loadings for Fe and Mn, linked to the negative redox conditions locally found in the region. Iron-manganese correlation is typical in anoxic groundwater, where these elements often show high concentration values due to the increased solubility of their oxides/hydroxides.

Last but not least, the fourth principal component explains the 9.8% of the total variance and features positive loadings for As and F, identifying the regional co-contamination object of this study.

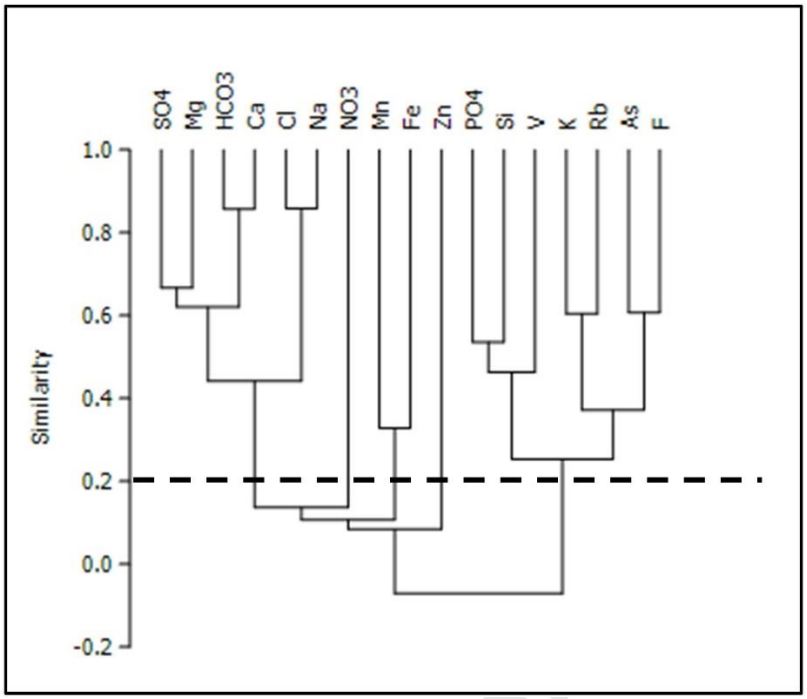

Fig. 4 – Dendrogram obtained with the application of hierarchical clustering to hydrochemical data.

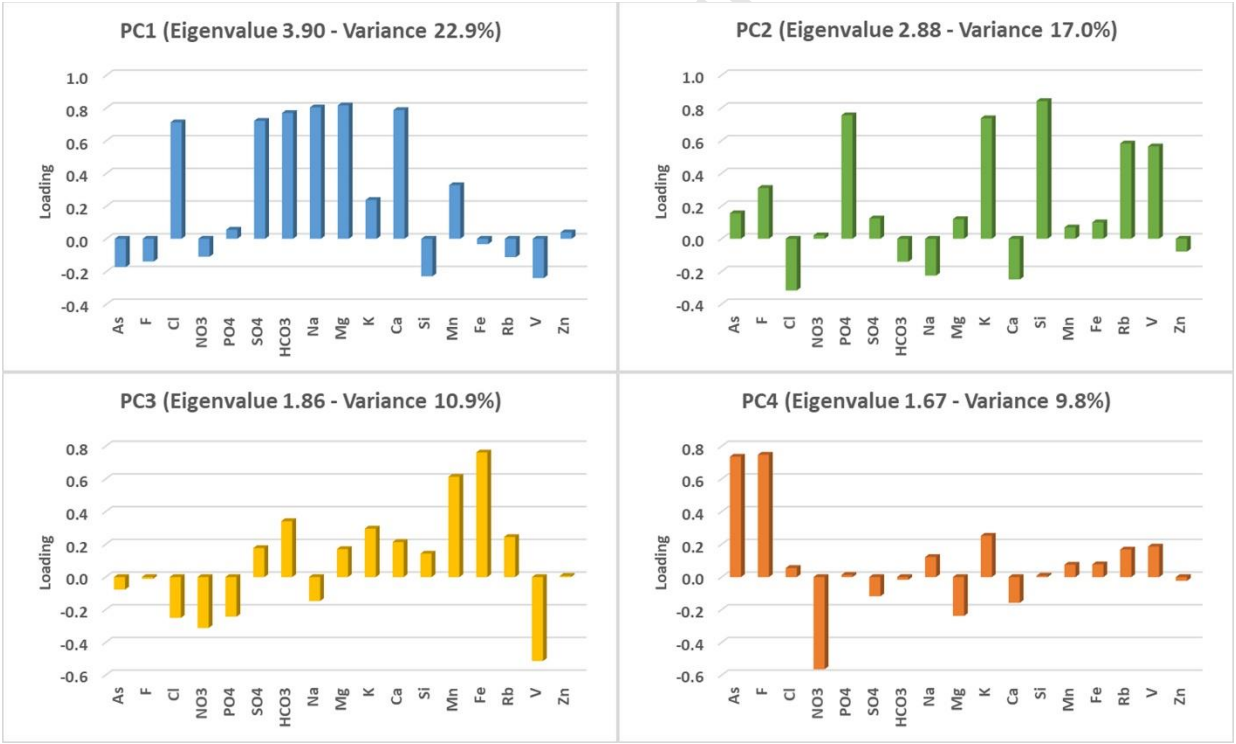

Fig. 5 – Principal Component Analysis: loadings for the four principal components (Factor rotation: Varimax normalized). Components with eigenvalues greater than 1 are shown.

The cumulative variance explained by the four principal components is 61.2%. Based on the results of the Piper classification, groundwaters were divided into two groups (group 1: Ca-waters; group 2: Mix/Na+K waters) and analyzed separately by PCA. The cumulative

variance slightly improves for the group 1, with four main components explaining 66.8% of the total variance. Cumulative variance is stable at 61.5% for the group 2. The variables that influence the two groups are substantially the same, with major ions on one side (PC1) and minor elements + K on the other (PC2). For group 2 there is a greater importance of the component linked to As-F (11.0% of the total variance), which becomes the third PC.

These results confirm that in the study area there is no clear limit between the two types of groundwaters, but rather a gradual transition of geochemical facies from the volcanic to the sedimentary domain. Overall, the analysis of the two separate water groups does not provide different results from those obtained by analyzing the entire dataset, which was therefore considered as a whole for the subsequent elaborations.

The normal Q-Q plots of both arsenic and fluoride show curved distributions while on a lognormal scale they are approximately linear in the central-upper range, especially fluoride (Fig. 6). However, their distribution is not normal nor lognormal (tested by Shapiro-Wilk test at a significance level = 0.05). Parrone et al. (2019) hypothesize that the Gaussian distribution of an element or compound in groundwater is representative of one single phenomenon, in principle responsible for the geochemical background, while any deviation from normality is due to other natural or anthropogenic processes. Probably this is what we observe here at a different scale. By definition, water-rock interaction processes determine the natural background of As and F. What on the local scale may appear to be an anomalous value, on a regional scale translates into one or more data populations derived from different processes acting in the investigated area, and overlap with the one representing the natural background. The spatial investigation described in the next paragraph aims at linking these anomalous values to the structural features of the study area.

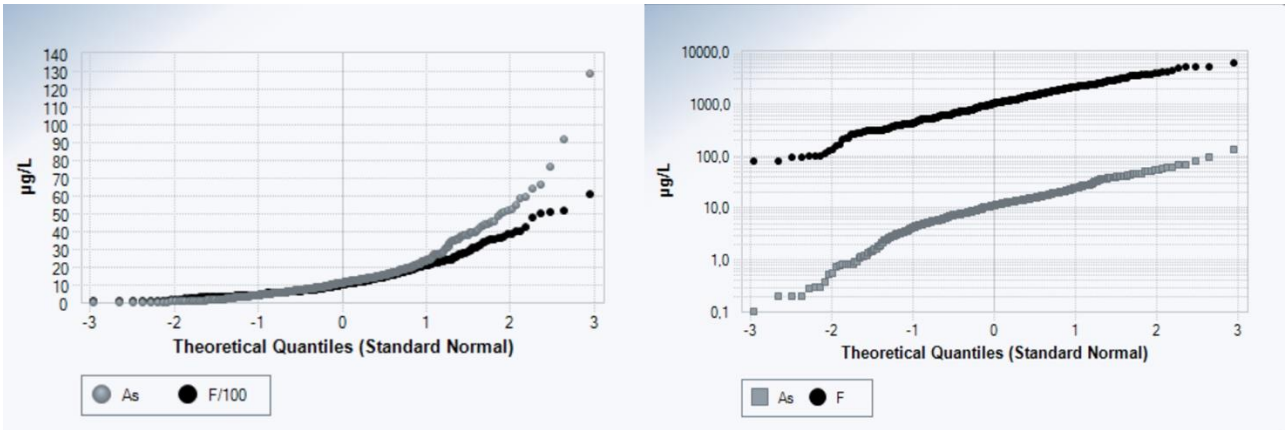

Fig. 6 – Normal (left) and lognormal (right) Q-Q plots for fluoride and arsenic.

3.2. As-F Kriging interpolation

The next step was to spatialize the As and F concentration data in order to analyze and compare their respective distribution in groundwater in the Northern Latium.

As and F prediction maps resulting from the application of the Ordinary Kriging (OK) are shown in Fig. 7. The model that best describes the experimental variograms is the spherical one. In both cases a Nugget Effect contributes to about the 30-33% of the structural variance.

The main parameters of the models that best fit all the experimental variograms for As, F and *r(As-F)* are reported in Table 3. The corresponding standard error maps related to all the spatial interpolations are included in the supplementary material (Fig. S1, S2 and S3).

The distribution of As and F in the survey area is not homogeneous; several concentration peaks are present, suggesting the existence of localized inputs. These could be related to the upwelling of thermal fluids along tectonic elements and to the consequent mixing phenomena in groundwater, as suggested by e.g. De Rita (2012) and Cinti et al (2015). The presence of ores of arsenic or fluoride bearing minerals, such as sulfides, fluoroapatite and fluorite, could also be invoked as a possible source for these localized inputs.

Regarding arsenic (Fig. 7a), the areas with the highest concentration are located to the south of the Bracciano Lake and in the central part of the Cimini-Vicani groundwater body, around the Vico Lake. Both lakes have settled into volcanic calderas. The concentration of arsenic decreases in the peripheral areas of the volcanic districts as well as along the Tyrrhenian coastal area, corresponding to the sedimentary domain. Further, among the three volcanic districts, the Vulsini one (to the North) shows lower As values on average.

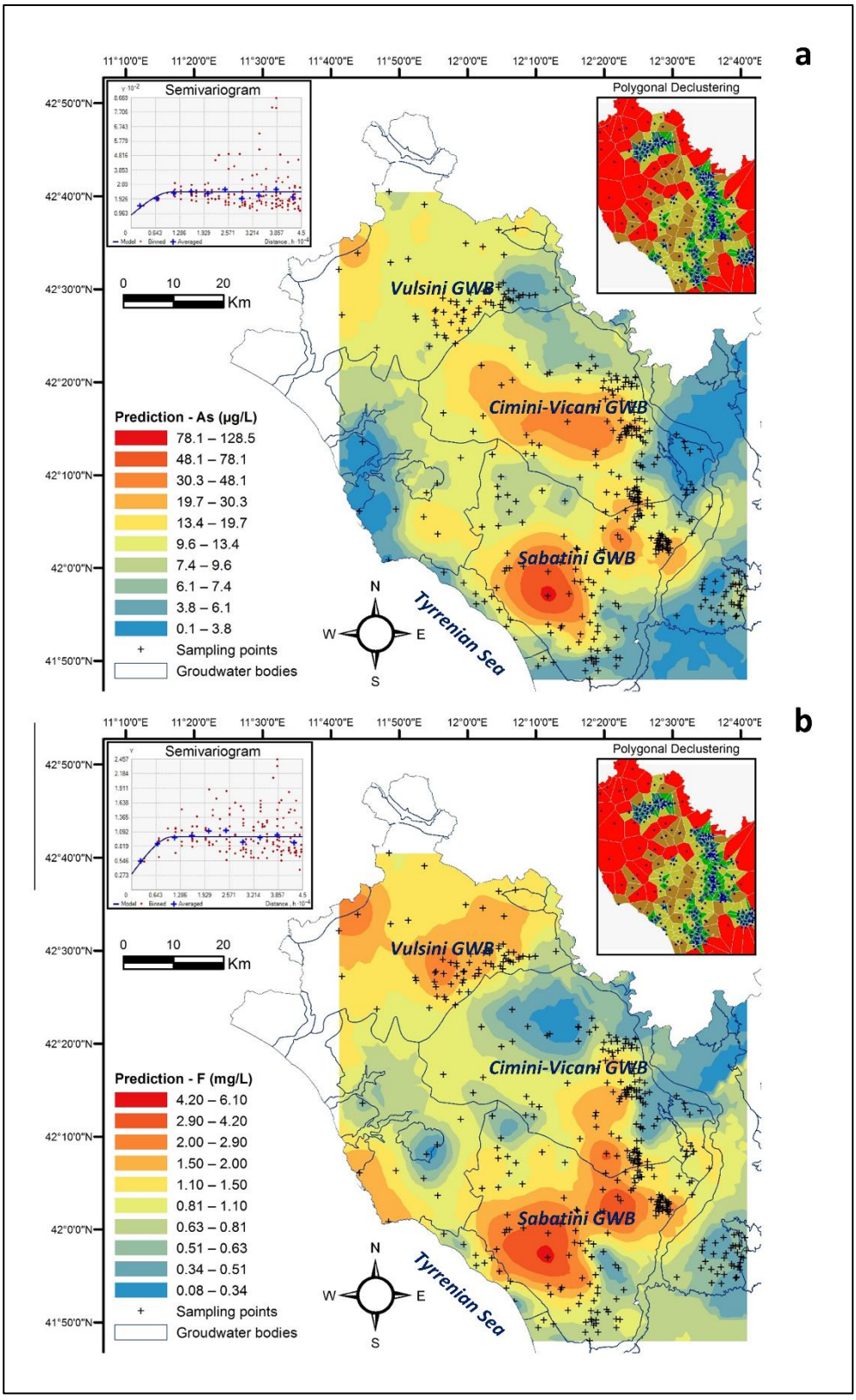

Fig. 7 – Ordinary Kriging results: Prediction Map for arsenic (a) and fluoride (b).

The highest concentrations of fluoride (Fig. 7b) have been found in the Vulsini GWB, in the Sabatini GWB and in the central coastal area, while lower values are located in the Vico Lake area and in the eastern periphery of the volcanic districts.

Regardless their origin and common geochemical processes, As and F are two elements of toxicological relevance, hence the areas where their concentrations can produce a significant risk to human health have been further investigated. In Fig. 8, the Indicator Kriging (IK) results show the probability to exceed the drinking water standards. For both parameters, the exponential model proved to be the most suitable for the experimental variograms. As done with OK, a Nugget Effect was added both for arsenic and for fluoride, representing 27-32% of the experimental variance.

The IK results show that groundwater resources exploitation for human consumption is critical with regard to arsenic in a large extent of the area (Fig. 8a). The situation might be better concerning fluoride (Fig. 8b) whose standard of 1.5 mg/L is largely exceeded only in the Sabatini groundwater body and in the northernmost area of the region.

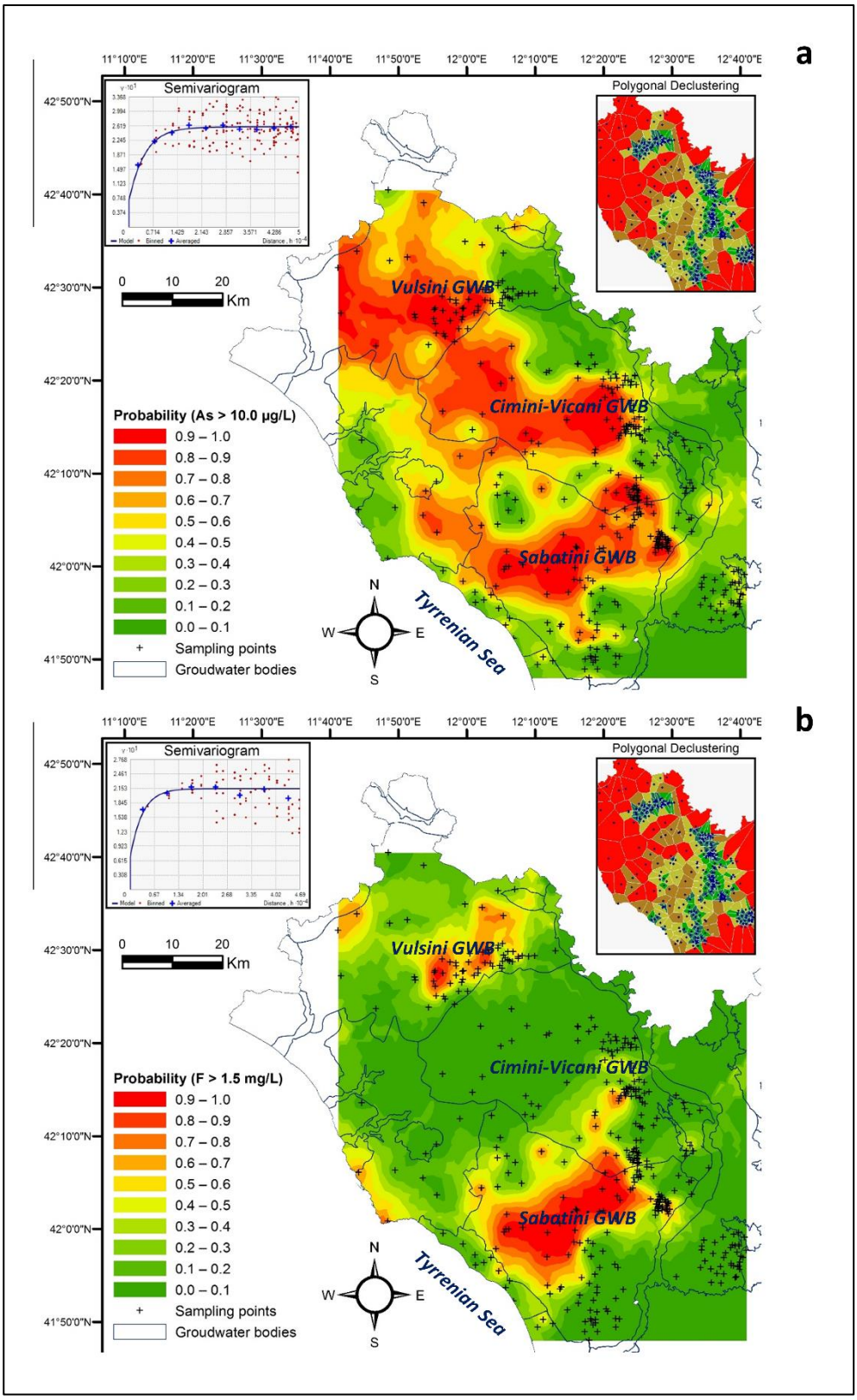

Fig. 8 – Indicator Kriging results: Probability Map for arsenic (a) and fluoride (b).

The concentration peaks shown in Fig. 7a (arsenic) and Fig. 7b (fluoride) are similar, but not completely overlapping. Hence, an increase in concentration for the one does not always imply a proportional increase for the other. The areas where As and F show individual fluctuations and their correlation decreases might indicate that other localized processes overlap, producing an increase of only one of the two elements, therefore reducing their correlation. In order to identify these areas, the jackknife technique was applied to the n (398) couples of As-F values and the obtained *r'* dataset was spatialized through IK in order to enhance where the two parameters are less correlated, hence the individual anomalies of one of the elements. In these cases, the exponential model resulted to be the most appropriate, combined with a Nugget Effect (21% of the variance).

In Fig. 9, green colors indicate a low probability of exceeding the threshold set for *r'*, hence the areas where the As-F correlation is more robust, while the brownish colors indicate the areas where the two parameters are less correlated; the blue/red crosses indicate an anomaly due to fluoride/arsenic.

For example, the concentration peak for arsenic identified in the central part of the Cimini-Vicani GWB and in the surroundings of the Vico Lake, corresponds to an anomaly for arsenic but not for fluoride. Anomalous zones for fluoride, but not for arsenic, are present in the eastern area of the Bracciano Lake, in the middle Tyrrhenian coastal area and in the southern part of the Vulsini GWB. The southeastern portion of the Sabatini groundwater body as well as the low Tyrrhenian coastal area, are characterized by several anomalous points for both arsenic and fluoride, even at a small distance from each other. On the other hand, at the edge of the volcanic districts, where the As-F concentrations are generically lower and groundwater geochemistry is increasingly affected by the sedimentary formations, the probability of exceeding the selected threshold value is always rather low, indicating that the correlation is more robust in this area.

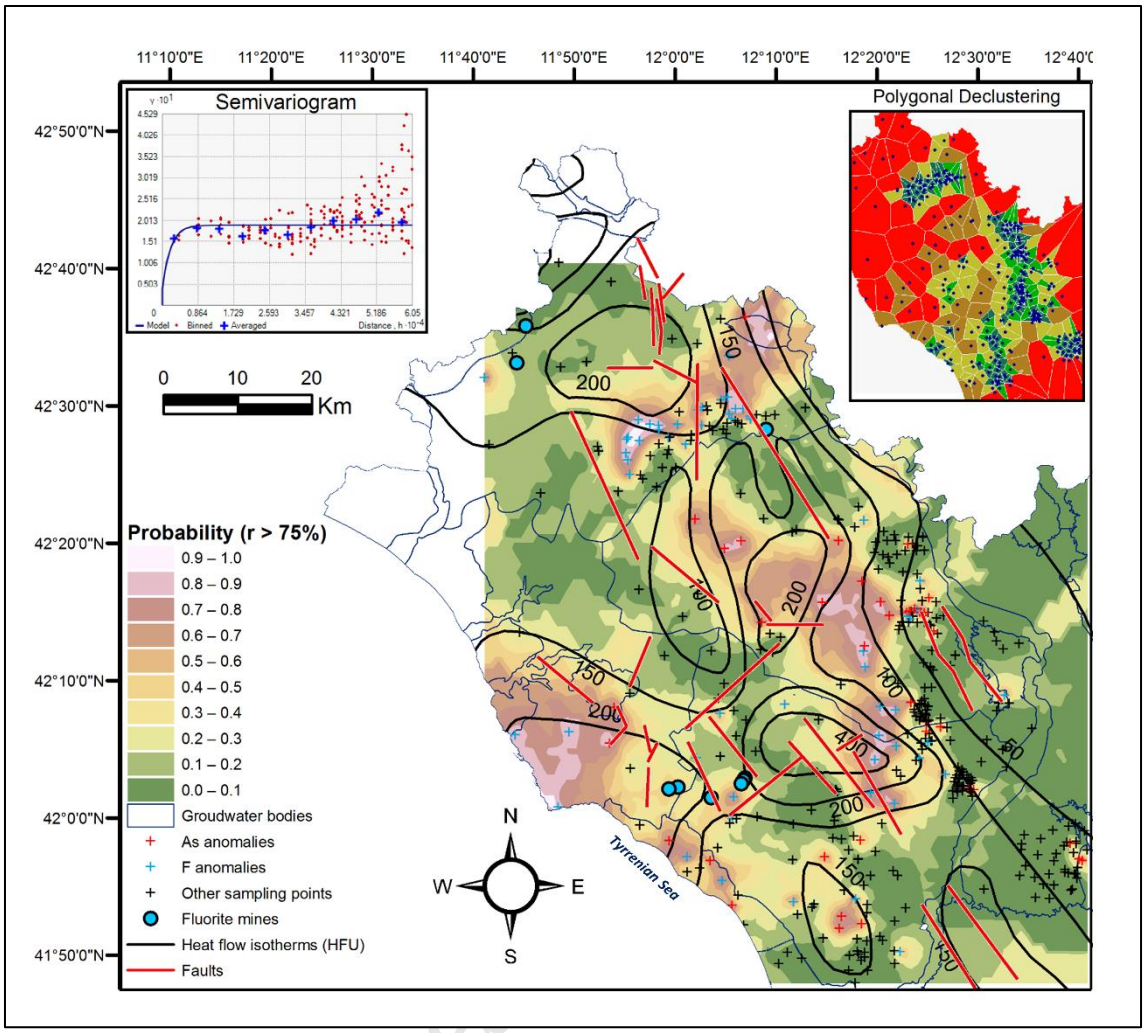

Fig. 9 – Indicator Kriging results: Probability Map for the resampled As-F correlation coefficient (r). Main faults are reported from Brunamonte et al. (1987).

Kriging Type	Variable	Threshold	Model		Range (a)
			C_0	C_1	
Ordinary	As	-	Nugget (80)	Spherical (160)	11000
	F	-	Nugget (0.3)	Spherical (0.7)	11000
Indicator	As	10.0	Nugget (0.07)	Exponential (0.19)	14000
	F	1.5	Nugget (0.07)	Exponential (0.15)	10000
	r (As-F)	0.608	Nugget (0.04)	Exponential (0.15)	6000

Table 3 – Main parameters of the models best-fitting the experimental variograms of As, F and r(As-F).

The main As-F correlation anomalies in Fig. 9 seem to correspond to the zones with the highest thermal flux, although slightly shifted from the peak area. In part, this could also be due to the uneven distribution of sampling points. In some cases, specific anomalies are

located near structural lineaments; this is evident for F, in particular to the east of Bracciano Lake and in the southern part of the Vulsini volcanic district. Further, the mining sites exploited in the past for fluorite cultivation near the Tyrrhenian coast are close to the anomaly for fluoride in the same area.

4. CONCLUSIONS

The main objective of this study was to investigate the processes responsible for the co-contamination of arsenic and fluoride in groundwater and to identify the most critical areas for the abstraction of drinking water supply.

The widespread geochemical background and the good correlation between the two elements observed in the study area points to a main process of interaction of cold groundwater with the volcanic formations on a regional scale. This process corresponds to the basal part of the QQ plot distribution. The correlation between arsenic and fluoride suggests that a common process maintains a geochemical equilibrium in groundwater; hence, we can expect that when the arsenic levels are high, fluoride is too. However, in certain areas, one of the two elements is more abundant in respect to the regional arsenic-fluoride correlation. Arsenic was found to be higher than expected in proximity to brittle elements, particularly those oriented NW-SE or at the intersection between NW-SE and NE-SW trending fractures and faults systems. Fluoride was found to be higher than expected around fluorite ores.

From a groundwater management point of view, the Indicator Kriging has proven effective for the assessment of the spatial probability of exceeding the drinking water standards for arsenic or fluoride, therefore it has allowed to identify those areas more/less convenient for the abstraction of water suitable for human consumption.

5. REFERENCES

Achene, L., Ferretti, E., Lucentini, L., Pettine, P., Veschetti, E., Ottaviani, M., 2010. Arsenic content in drinking-water supplies of an important volcanic aquifer in central Italy. Toxicol. Environ. Chemistry 92, 509-520.

Aiuppa, A., D'Alessandro, W., Federico, C., Palumbo, B., Valenza, M., 2003. The aquatic geochemistry of arsenic in volcanic groundwaters from southern Italy. Appl. Geochem. 18, 1283-1296.

Alarcón-Herrera, M.T., Bundschuh, J., Nath, B., Nicolli, H.B., Gutierrez, M., Reyes-Gomez, V.M., Nu˜nez, D., Martín-Dominguez, I.R., Sracek, O., 2013. Co-occurrence of arsenic and fluoride in groundwater of semi-arid regions in Latin America: Genesis, mobility and remediation. Journal of Hazardous Materials 262, 960– 969.

Anawar, H.M, Akai, J., Komaki, K., Terao, H., Takahito Yoshiokae, Ishizuka, T., Safiullah, S., Kato, K., 2003. Geochemical occurrence of arsenic in groundwater of Bangladesh: sources and mobilization processes. J. Geochem. Explor. 77, 109.131.

Angelone, M., Cremisini, C., Piscopo, V., Proposito, M., Spaziani, F., 2009. Influence of hydrostratigraphy and structural setting on the arsenic occurrence in groundwater of the Cimino-Vico volcanic area (Central Italy). Hydrogeol. J. 17, 901-914.

Armienta, M.A., Segovia, N., 2008. Arsenic and fluoride in the groundwater of Mexico. Environ. Geochem. Health 30, 345–353.

Armiento, G., Baiocchi, A., Cremisini, C., Crovato, C., Lotti, F., Lucentini, L., Mazzuoli, M., Nardi, E., Piscopo, V., Proposito M., Veschetti, E., 2015. An Integrated Approach to Identify Water Resources for Human Consumption in an Area Affected by High Natural Arsenic Content. Water 7, 5091-5114.

Baiocchi, A., Coletta, A., Espositi, L., Lotti F., Piscopo V., 2013. Sustainable groundwater development in a naturally arsenic-contaminated aquifer: The case of the Cimino-Vico volcanic area (central Italy). Ital. J. Eng. Geol. Environ. 1, 5-18.

Bangsund, W.J., Peng, C.G., Mattsfield, W.R., 1994. Investigation of contaminant migration by low-flow rate sampling techniques. Proceedings of the Eighth Annual Outdoor Action Conference, National Groundwater Association, Dublin, OH, pp. 311-326.

BGS, 2019a. Arsenic contamination of groundwater. https://www.bgs.ac.uk/research/groundwater/health/arsenic/home.html.

BGS, 2019b. Fluoride in Groundwater. http://www.bgs.ac.uk/research/groundwater/health/fluoride.html.

Bhattacharya, P., Claesson, M., Bundschuh, J., Srack, O., Fagerberg, J., Jacks, G., Martin, R.A., Storniolo Adel, R., Thir, J.M., 2006. Distribution and mobility of Arsenic in the Rio Dulce Alluvial aquifers in Santiago del Estero Province, Argentina. Sci. Total Environ. 358, 97-120.

Boni, C., Bono, P., Capelli, G., 1988. Carta idrogeologica del territorio della Regione Lazio. Scala 1:250.000. Pubblicazione Speciale Regione Lazio Vol. Unico. Roma: Regione Lazio (Italy).

Brindha, K., Elango, L., 2011. Fluoride in Groundwater: Causes, Implications and Mitigation Measures, In: Monroy, S.D. (Ed.), Fluoride Properties, Applications and Environmental Management. pp. 111–136.

Brunamonte F., Cosentino D., D'Amico L., Gavasci R., Prestininzi A., Romagnoli C., 1987. Carta dei sistemi idrogeologici del Territorio della Regione Lazio. Scala 1:200.000. Regione Lazio - Università degli Studi di Roma "La Sapienza", Roma.

Brunt, R., Vasak, L., Griffioen, J., 2004. Fluoride in groundwater: Probability of occurrence of excessive concentration on global scale. International Groundwater Resources Assessment Centre Report, SP 2004-2.

Bundschuh, J., Litter, M., Parvez, F., Román-Ross, G., Nicolli, H., Jean, J., et al., 2012. One century of arsenic exposure in Latin America: a review of history and occurrence from 14 countries. Sci. Total Environ. 429, 2-35.

Cinti, D., Procesi, M., Tassi, F., Montegrossi, G., Sciarra, A., Vaselli, O., Quattrocchi, F., 2011. Fluid geochemistry and geothermometry in the western sector of the Sabatini Volcanic District and the Tolfa Mountains (Central Italy). Chem. Geol. 284, 160–181.

Cinti, D., Poncia, P.P., Brusca, L., Tassi, F., Quattrocchi, F., Vaselli, O., 2015. Spatial distribution of arsenic, uranium and vanadium in the volcanic-sedimentary aquifers of the Vicano–Cimino Volcanic District (Central Italy). J. Geochem. Explor. 152, 123–133.

Claesson, M., Fagerberg, J., 2003. Arsenic in groundwater of Santiago del Estero, Argentina. Sources, mobilization, controls and remediation with natural materials. Minor Field Studies Scholarship Programme MFS, Royal Institute of Technology (KTH), Stockholm.

Cubadda F., D'Amato M., Mancini F.R., Aureli F., Raggi A., Busani L., Mantovani A. 2015. Assessing human exposure to inorganic arsenic in high-arsenic areas of Latium: a biomonitoring study integrated with indicators of dietary intake. Ann. Di Ig. 27, 39-51. https://doi.org/10.7416/ai.2015.2021

Currell, M., Cartwright, I., Raveggi, M., Han, D., 2011. Controls on elevated fluoride and arsenic concentrations in groundwater from the Yuncheng Basin, China. Appl. Geochem. 26, 540-552.

Dall'Aglio, M., Duchi, V., Minissale, A., Guerrini, A., Tremori, M., 1994. Hydrogeochemistry of the volcanic district in the Tolfa and Sabatini Mountains in central Italy. J. Hydrol. 154, 195–217.

Dall'Aglio, M., Giuliano, G., Amicizia, D., Andrenelli, M.C., Cicioni, G.B., Mastroianni, D., Sepicacchi, L., Tersigni, S., 2001. Assessing drinking water quality in Northern Latium by trace elements analysis. Proceedings of water rock interaction (WRI-10), International Congress, vol 2, 1063–1066.

Daniele, L., 2004. Distribution of arsenic and other minor trace elements in the groundwater of Ischia Island. Environ. Geol. 46, 96–103. https://doi.org/10.1007/s00254-

004-1018-z

De Rita, D., Cremisini, C., Cinnirella, A., Spaziano, F., 2012. Fluorine in the rocks and sediments of volcanic area in central Italy: total content, enrichment and leaching process and a hypothesis on the vulnerability of the related aquifers. Environ. Monit. Assess. 184, 5781–5796

EC Directive, 1998. Council Directive 98/83/EC of 3 November 1998 on the quality of water intended for human consumption. European Commission, Brussels.

Edmunds, W.M., Smedley, P.L. 2013. Fluoride in Natural Waters. In: Selinus O. (eds) Essentials of Medical Geology. Springer, Dordrecht

Efron, B., Stein, C., 1981. The Jackknife Estimate of Variance. The Annals of Statistics. 9 (3), 586–596.

EPA U.S., 2002. Calculating Upper Confidence Limits for Exposure Point Concentrations at Hazardous Waste Sites [Supplemental Guidance to RAGS.] OSWER Directive 9285.6-10. Washington, DC, USA.

Finetti, I., Del Ben, A., 1986. Geophysical study of the Tyrrhenian opening. Boll. Geof. Teor. Appl. 28, 75-156.

Ford, R.G., Fendorf, S., Wilkin, R.T., 2006. Introduction: Controls on arsenic transport in near-surface aquatic systems. Chem. Geol. 228, 1–5.

Francisca, F.M., Carro Perez, M.E., 2009. Assessment of natural arsenic in groundwater in Cordoba Province, Argentina. Environ. Geochem. Hlth. 31, 673–682.

Gaus, I., Kinniburgh, D.G., Talbot, J.C., Webster, R., 2003. Geostatistical analysis of arsenic concentration in groundwater in Bangladesh using disjunctive kriging. Env. Geol. 44, 939-948.

Gomez, M.L., Blarasin, M.T., Martinez, D.E., 2009. Arsenic and fluoride in a loess aquifer in the central area of Argentina. Environ. Geol. 57(1), 143-155.

Guo, H., Zhang, Y., Xing, L., Jia, Y., 2012. Spatial variation in arsenic and fluoride concentrations of shallow groundwater from the town of Shahai in the Hetao basin, Inner Mongolia. Appl. Geochem. 27, 2187-2196.

Hammer, Ø., Harper, D.A.T., Ryan, P.D., 2001. PAST: Paleontological statistics software

Karim, M.M., 2000. Arsenic in groundwater and health problems in Bangladesh. Wat. Res. 34, 304-310.

Kim, S.H., Kim, K., Ko, K.S., Kim, Y., Lee, K.S., 2012. Co-contamination of arsenic and fluoride in the groundwater of unconsolidated aquifers under reducing environments. Chemosphere 87, 851-856.

Levy, D.B., Schramke, J.A., Esposito, K.J., Erickson, T.A., Moore, J.C., 1999. The shallow ground water chemistry of arsenic, fluorine, and major elements: Eastern Owens Lake, California. Appl. Geochem. 14(1), 53-65.

Lin, Y.P., Chang, T.K., Shih, C.W., Tseng, C.H., 2002. Factorial and indicator kriging methods using a geographic information system to delineate spatial variation and pollution sources of soil heavy metals. Env. Geol. 42, 900–909.

Locardi, E., 1982. Individuazione delle strutture sismogenetiche dall'esame dell'evoluzione vulcano-tettonica dell'Appennino e del Tirreno. Mem. Soc. Geo. It. 24, 569-596.

McArthur, J.M., Banerjee, D.M., Hudson-Edwards, K.A., Mishra, R., Purohit, R., Ravenscroft, P., Cronin, A., Howarth, R.J., Chatterjee, A., Talukder, T., Lowry, D., Houghton, S., Chadha D.K., 2004. Natural organic matter in sedimentary basins and its relation to arsenic in anoxic ground water: the example of West Bengal and its worldwide implications. Appl. Geochem. 19, 1255-1293.

Morales, I., Villanueva-Estrada, R.E., Rodríguez, R., Armienta, M.A., 2015. Geological, hydrogeological, and geothermal factors associated to the origin of arsenic, fluoride, and groundwater temperature in a volcanic environment "El Bajío Guanajuatense", Mexico. Environ. Earth Sci. 74, 5403-5415.

Mukherjee A, Verma S, Gupta S, Henke K.R., Bhattacharya P (2014) Influence of tectonics, sedimentation and aqueous flow cycles on the origin of global groundwater arsenic: Paradigms from three continents. Journal of Hydrology 518, 284–299.

Nickson, R., McArthur, J.M., Ravencroft, P., Burgess, W.G., Ahmed, K.M., 2000. Mechanism of arsenic release to groundwater, Bangladesh and West Bengal. Appl. Geochem. 15, 403–413.

Nicolli, H.B., Suriano, J.M., Gomez Peral, M.A., Ferpozzi, O.A., Baleani, O.A., 1989. Groundwater contamination with arsenic and other trace elements in an area of the Pampa, Province of Cordoba, Argentina. Environ. Geol. Water Sci. 14, 3–16.

Nicolli, H.B., Tineo, A., Garcia, J.W., Falcon, C.M., Merino M.H., 2001. Trace-element quality problems in groundwater from Tucuman, Argentina. Cidu R (ed) Proc of the 10th International Symposium on Water Rock Interaction WRI-10, Villasimius, Italy, 10–15 July 2001, pp 993–996.

Nicolli, H.B., Garcia J.W., Falcon, C.M., Smedley, P.L., 2012. Mobilization of arsenic and other trace elements of health concern in groundwater from the Salì River Basin, Tucuman Province, Argentina. Environ. Geochem. Health. 34, 251–262.

Parrone D., Preziosi, E., Del Bon A., Ghergo, S., 2013. Hydrogeochemical characterization of a volcanic-sedimentary aquifer in Central Italy. Rend. Online Soc. Geol. It. 24, 232-234.

Parrone D., Ghergo S., Preziosi E. 2019. A multi-method approach for the assessment of natural background levels in groundwater. Sci. Total Environ. 659, 884-894.

Pazand, K., Javanshir, A.R., 2013. Hydrogeochemistry and arsenic contamination of groundwater in the Rayen area, southeastern Iran. Environ. Earth. Sci. 70, 2633–2644.

Peccerillo, A., 2005. Plio-Quaternary Volcanism in Italy. Petrology, geochemistry, geodynamics. Springer, Heidelberg, p 365

Pohlman, K.F., Icopini, G.A., McArthur, R.D., Rosal, C.G., 1994. Evaluation of sampling and field-filtration methods for the analysis of trace metals in ground water. EPA/600/R-94/119.

Preziosi, E., Vivona, R., Giuliano, G., 2005. Microinquinanti di origine naturale negli acquiferi vulcanici: un approccio integrato quantitative e qualitativo nel Lazio settentrionale [Micropollutants of natural origin in volcanic aquifers: an integrated quantitative and qualitative approach in northern Latium]. IGEA 20, 3–14.

Preziosi, E., Giuliano, G., Vivona, R., 2010. Natural background levels and threshold values derivation for naturally As, V and F rich groundwater bodies: a methodological case study in Central Italy. Environ. Earth. Sci. 61, 885–897.

Preziosi, E., Parrone, D., Del Bon, A., Ghergo, S., 2014. Natural background level assessment in groundwaters: probability plot versus pre-selection method. J. Geochem. Explor. 143, 43-53.

Preziosi, E., Rossi, D., Parrone, D., Ghergo, S., 2015. Groundwater chemical status assessment considering geochemical background: an example from Northern Latium (Central Italy). Rend. Fis. Acc. Lincei 27(1), 59-66.

Preziosi E., Frollini E., Zoppini A., Ghergo S., Melita M., Parrone D., Rossi D., Amalfitano S., 2019. Disentangling natural and anthropogenic impacts on groundwater by hydrogeochemical, isotopic and microbiological data: Hints from a municipal solid waste landfill. Waste Manag. 84, 245-255.

Quenouille, M.H., 1949. Problems in Plane Sampling. The Annals of Mathematical Statistics. 20(3), 355–375.

Quenouille, M.H., 1956. Notes on Bias in Estimation. Biometrika. 43 (3-4), 353–360.

Rango, T., Vengosh, A., Dwyer, G., Bianchini, G., 2013. Mobilization of arsenic and other naturally occurring contaminants in groundwater of the Main Ethiopian Rift aquifers. Water Res. 47, 5801–5818.

Rossman, T.G., Uddin, A.N., Burns, F.J., 2004. Evidence that arsenite acts as a cocarcinogen in skin cancer. Toxicol. Appl. Pharmacol. 198, 394–404.

Shapiro, S.S., Wilk, M.B., 1965. An analysis of variance test for normality (complete samples). Biometrika, 52 (3-4), p. 591

Singh, A., Maichle, R., 2013. ProUCL Version 5.0.00 User Guide-Statistical Software for Environmental Applications for Data Sets with and without Nondetect Observations. EPA: Washington, WA, USA.

Smedley, P.L., Nicolli, H.B., Macdonald, D.M.J., Barros, A.J., Tullio, J.O., 2002. Hydrogeochemistry of arsenic in groundwater from La Pampa, Argentina. Appl. Geochem. 17, 259–284.

Smedley, P.L., Kinniburgh, D.G., 2002. A review of the source, behavior and distribution of arsenic in natural waters. Appl. Geochem. 17, 517–568.

Smedley, P.L., 2008. Sources and distribution of arsenic in groundwater. In: T. Appelo and J.P. Heederik, Arsenic in Groundwater – a world problem, Utrecht Seminar NNC-IAH, November 2006, Utrecht, The Netherlands.

StatSoft Inc., 2004. STATISTICA (data analysis software system), version 7. www.statsoft.com.

Tchounwou, P.B., Centeno, J.A., Patlolla, A.K., 2004. Arsenic toxicity, mutagenesis, and carcinogenesis—a health risk assessment and management approach. Mol. Cell. Biochem. 255, 47–55.

Tukey, J.W., 1958. Bias and confidence in not quite large samples. The Annals of Mathematical Statistics. 29, 614–623.

USEPA, 2002. Calculating Upper Confidence Limits for Exposure Point Concentrations at Hazardous Waste Sites. OSWER 9285.6-10.

Vivona, R., Preziosi, E., Giuliano, G., Mastroianni, D., Falconi, F., Madé, B., 2004. Geochemical characterization of a volcanic-sedimentary aquifer in Central Italy. Wanty R,

Seal R II (eds) Proc. of the 11th International Symposium on Water-Rock Interaction WRI-11, Saratoga Springs, New York, June 2004, pp 513–517.

Vivona, R., Preziosi, E., Madé, B., Giuliano, G., 2007. Occurrence of minor toxic elements in volcanic-sedimentary aquifers: a case study in central Italy. Hydrogeol J. 15, 1183-1196.

Wezel, F.C., 1982. The Tyrrhenian Sea: a rifted Krikogenic-swell basin. Mem. Descr. Carta Geol. It. 24, 532-568.

WHO, 2017. Guidelines for drinking-water quality - 4th ed., incorporating the 1st addendum. ISBN: 978-92-4-154995-0. World Health Organisation, Geneva, Switzerland.

Yang, Q., Jung, H.B., Culbertson, C.W., Marvinney, R.G., Loiselle, M.C., Locke, D.B., Cheek, H., Thibodeau, H., Zheng, Y., 2009. Spatial pattern of groundwater arsenic occurrence and association with bedrock geology in greater Augusta, Maine. Environ. Sci. Technol. 43(8), 2714–2719.

Yoshida, T., Yamauchi, H., Fan Sun G., 2004. Chronic health effects in people exposed to arsenic via the drinking water: dose-response relationships in review. Toxicol. Appl. Pharmacol. 198(3), 243-52.

Supplementary material

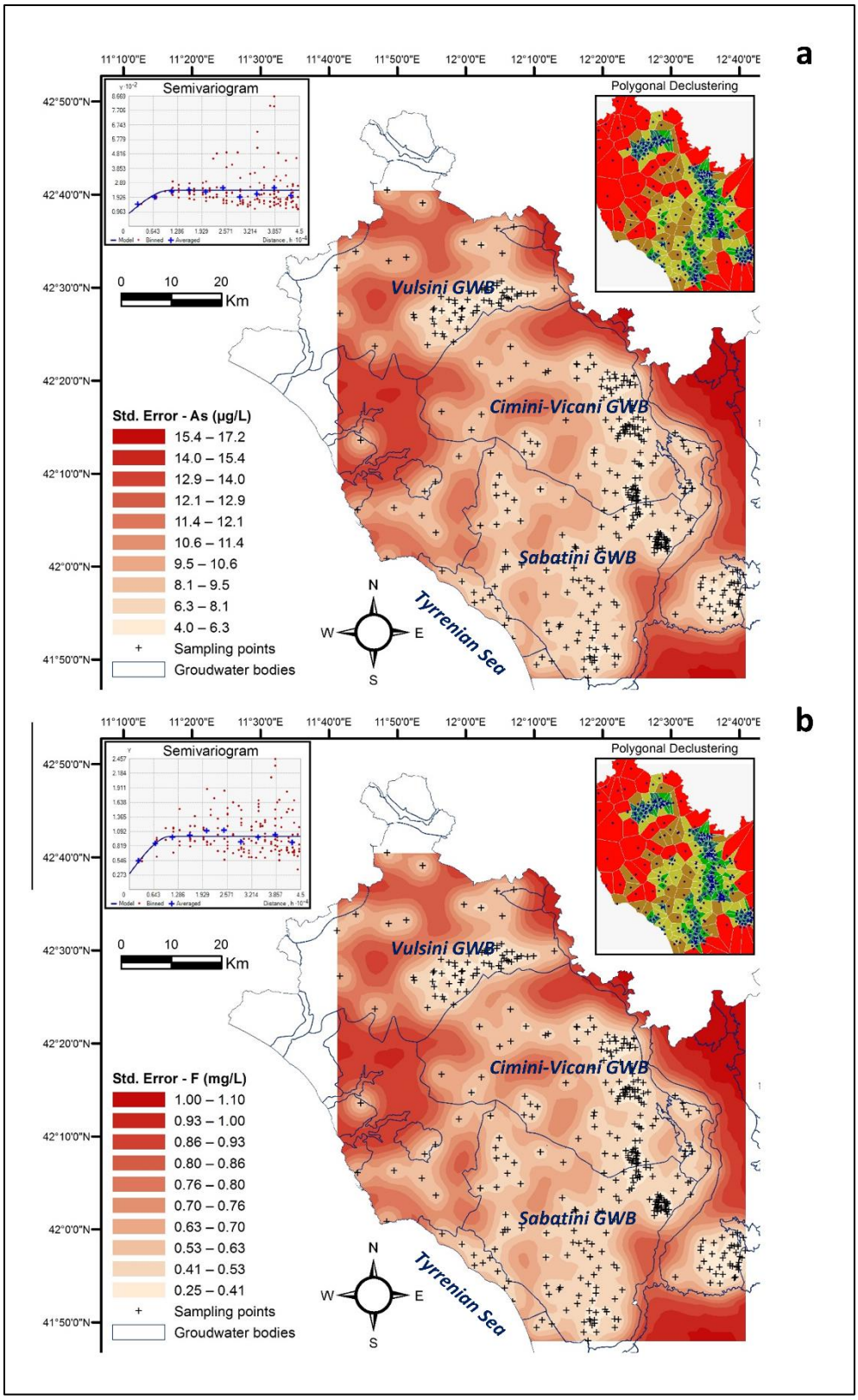

Fig. S1 – Ordinary Kriging results: Standard Error Map for arsenic (a) and fluoride (b).

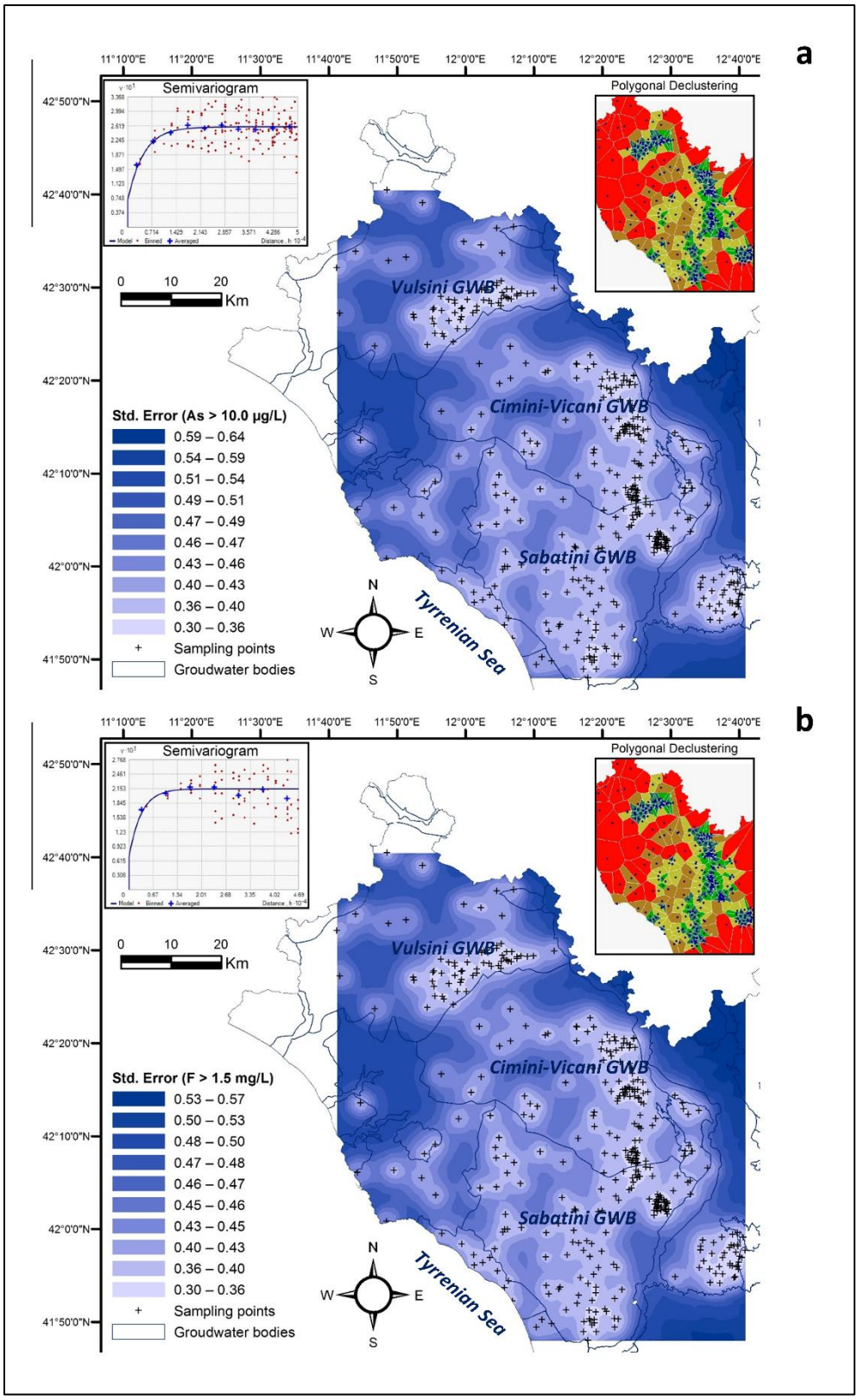

Fig. S2 – Indicator Kriging results: Standard Error Map for arsenic (a) and fluoride (b).

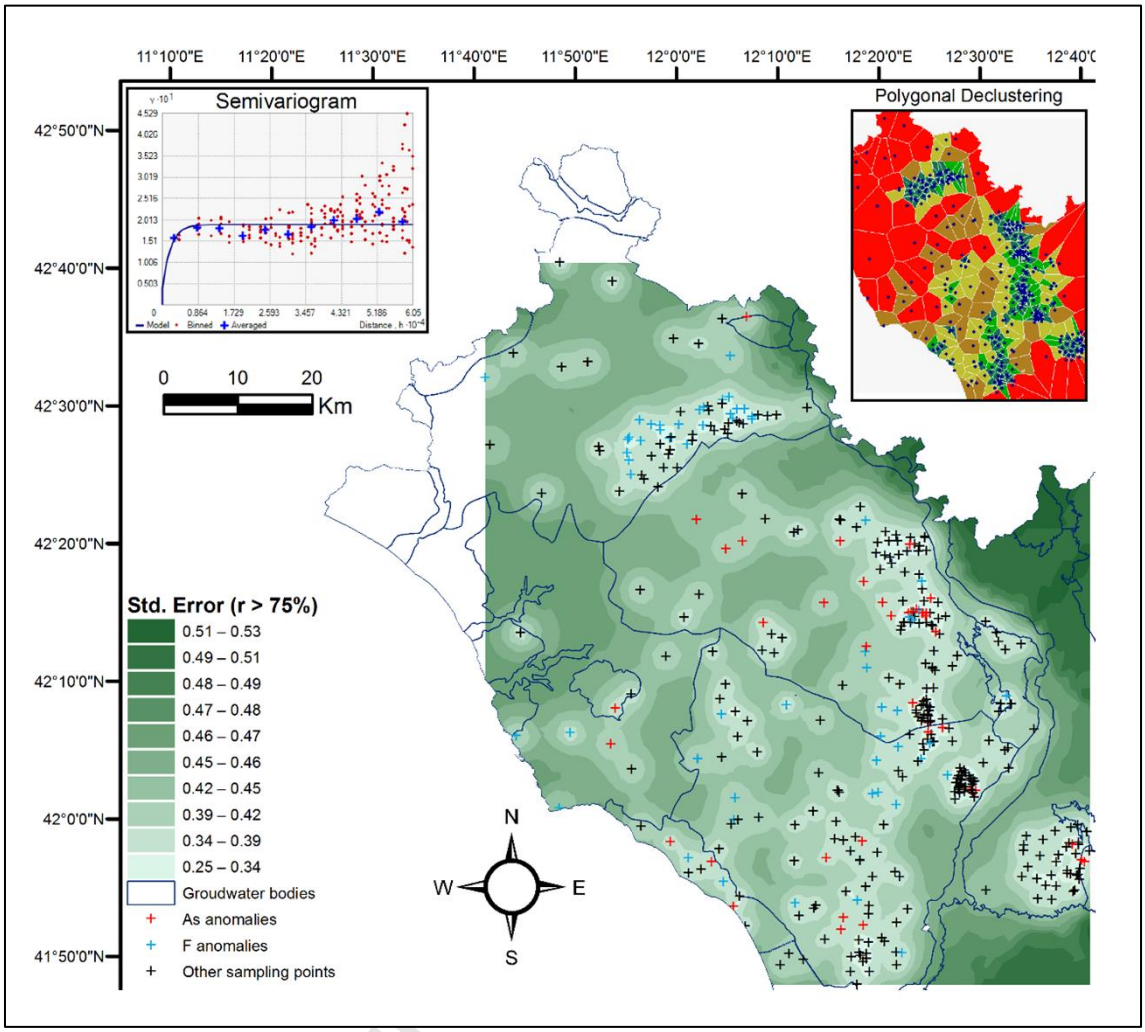

Fig. S3 – Indicator Kriging results: Standard Error Map for the resampled As-F correlation coefficient (r).

Credit author statement

Daniele Parrone: Conceptualization, Methodology, Formal analysis, Writing - Original Draft, Writing - Review & Editing
Stefano Ghergo: Conceptualization, Writing - Review & Editing
Eleonora Frollini: Data Curation, Writing - Review & Editing,
David Rossi: Writing - Review & Editing
Elisabetta Preziosi: Conceptualization, Writing - Review & Editing,

Declaration of interests

☒ The authors declare that they have no known competing financial interests or personal relationships that could have appeared to influence the work reported in this paper.

☐The authors declare the following financial interests/personal relationships which may be considered as potential competing interests:

Parameter	Samples	Min	Max	Mean	Median	VC%	Skewness	Kurtosis
ORP (mV)	385	-323	669	188	200	0.5	-0.3	3.9
T (°C)	398	5.3	25.7	16.6	16.5	0.1	0.0	3.5
pH	396	5.4	8.6	7.0	7.1	0.1	-0.6	0.0
DO (mg/L)	397	0.0	21.3	6.7	7.2	0.5	0.1	0.9
Cond (µS/cm)	317	216	2930	695	597	0.6	2.8	10.3
F (mg/L)	398	0.1	6.1	1.2	1.0	0.8	1.7	3.7
Cl (mg/L)	398	4.2	619.0	37.4	24.0	1.4	6.6	57.5
NO_3 (mg/L)	398	0.1	244.9	25.6	16.6	1.2	3.8	20.0
PO_4 (mg/L)	352	0.003	4.16	0.4	0.3	1.3	2.7	10.5
SO_4 (mg/L)	398	2.0	1018.6	41.6	17.1	2.0	6.3	58.8
HCO_3 (mg/L)	398	31.4	1281.0	288.5	246.4	0.6	2.0	7.2
Na (mg/L)	398	2.5	548.7	38.0	27.8	1.0	6.9	73.1
Mg (mg/L)	398	2.6	132.0	15.6	12.0	0.9	3.5	18.9
K (mg/L)	398	0.2	209.2	27.2	23.4	0.9	3.1	16.6
Ca (mg/L)	398	1.8	420.9	69.7	48.6	0.9	2.3	6.9
Si (mg/L)	364	2.0	58.3	28.9	28.9	0.4	0.0	-0.3
Mn (µg/L)	371	0.02	3577.7	88.7	2.3	3.9	6.5	49.3
Fe (µg/L)	337	0.3	7614.0	187.5	16.4	4.4	6.5	44.2
As (µg/L)	398	0.1	128.5	14.4	11.0	1.0	2.9	14.0
Rb (µg/L)	365	0.2	313.8	53.5	45.2	0.8	2.4	8.1
V (µg/L)	398	0.1	99.4	19.8	16.5	0.8	1.1	1.7
Zn (µg/L)	395	0.2	2470.0	54.8	14.8	3.2	9.5	112.1

Table 1 – Main statistics for the considered parameters.

	F	Cl	NO_3	PO_4	SO_4	HCO_3	Na	Mg	K	Ca	Si	Mn	Fe	Rb	V	Zn	As
F																	
Cl	-0.17																
NO_3	-0.20	0.17															
PO_4	**0.21**	**-0.35**	0.11														
SO_4	-0.14	**0.61**	0.13	**-0.21**													
HCO_3	-0.12	**0.57**	-0.18	**-0.37**	**0.55**												
Na	0.07	**0.73**	0.01	-0.19	**0.62**	**0.66**											
Mg	**-0.24**	**0.57**	0.05	-0.09	**0.61**	**0.70**	**0.62**										
K	**0.61**	**-0.21**	**-0.25**	**0.40**	-0.16	-0.08	0.07	-0.12									
Ca	**-0.28**	**0.63**	0.01	**-0.41**	**0.62**	**0.89**	**0.59**	**0.64**	**-0.28**								
Si	**0.29**	**-0.36**	0.06	**0.71**	**-0.22**	**-0.36**	-0.16	-0.10	**0.54**	**-0.43**							
Mn	0.08	0.11	**-0.32**	0.02	**0.28**	**0.32**	**0.29**	**0.30**	**0.22**	**0.25**	0.09						
Fe	0.05	0.12	**-0.20**	-0.07	**0.26**	**0.22**	0.17	**0.21**	0.12	**0.21**	-0.03	**0.56**					
Rb	**0.39**	**-0.36**	-0.01	**0.51**	**-0.21**	**-0.32**	-0.13	**-0.22**	**0.58**	**-0.37**	**0.59**	0.09	0.01				
V	**0.35**	**-0.30**	**0.23**	**0.58**	**-0.44**	**-0.42**	**-0.23**	**-0.24**	**0.37**	**-0.47**	**0.49**	**-0.25**	**-0.23**	**0.34**			
Zn	0.03	0.14	0.09	-0.10	0.13	0.11	0.11	0.09	0.00	0.14	-0.12	**0.24**	0.18	-0.03	-0.15		
As	**0.59**	**-0.26**	-0.17	**0.30**	**-0.29**	**-0.27**	-0.03	**-0.42**	**0.46**	**-0.37**	**0.33**	-0.01	-0.07	**0.44**	**0.42**	-0.09	

Table 2 – Spearman (r_S) correlation coefficients for the analyzed parameters. Statistically significant values in bold (α = 0.001).

Kriging Type	Variable	Threshold	Model		Range (a)
			C_0	C_1	
Ordinary	As	-	Nugget (80)	Spherical (160)	11000
	F	-	Nugget (0.3)	Spherical (0.7)	11000
Indicator	As	10.0	Nugget (0.07)	Exponential (0.19)	14000
	F	1.5	Nugget (0.07)	Exponential (0.15)	10000
	r (As-F)	0.608	Nugget (0.04)	Exponential (0.15)	6000

Table 3 – Main parameters of the models best-fitting the experimental variograms of As, F and r(As-F).

Highlights

- Arsenic-fluoride correlation in a volcanic-sedimentary aquifer in Italy is analyzed
- Water-rock interaction produces the As-F background and maintains their correlation
- Anomalies appear linked to interaction with geothermal fluids and/or mineral deposits
- Indicator kriging indicates the most suitable areas for drinking water exploitation